UCRL-JC-127279
PREPRINT

Numerical Simulation of Ultra-Short Laser Pulse Energy Deposition and Transport for Material Processing

A. M. Rubenchik
M. D. Feit
M. D. Perry
J. T. Larsen

This paper was prepared for submittal to the
Fourth Conference on Laser Ablation
Pacific Grove, CA
July 21-25, 1997

July 18, 1997

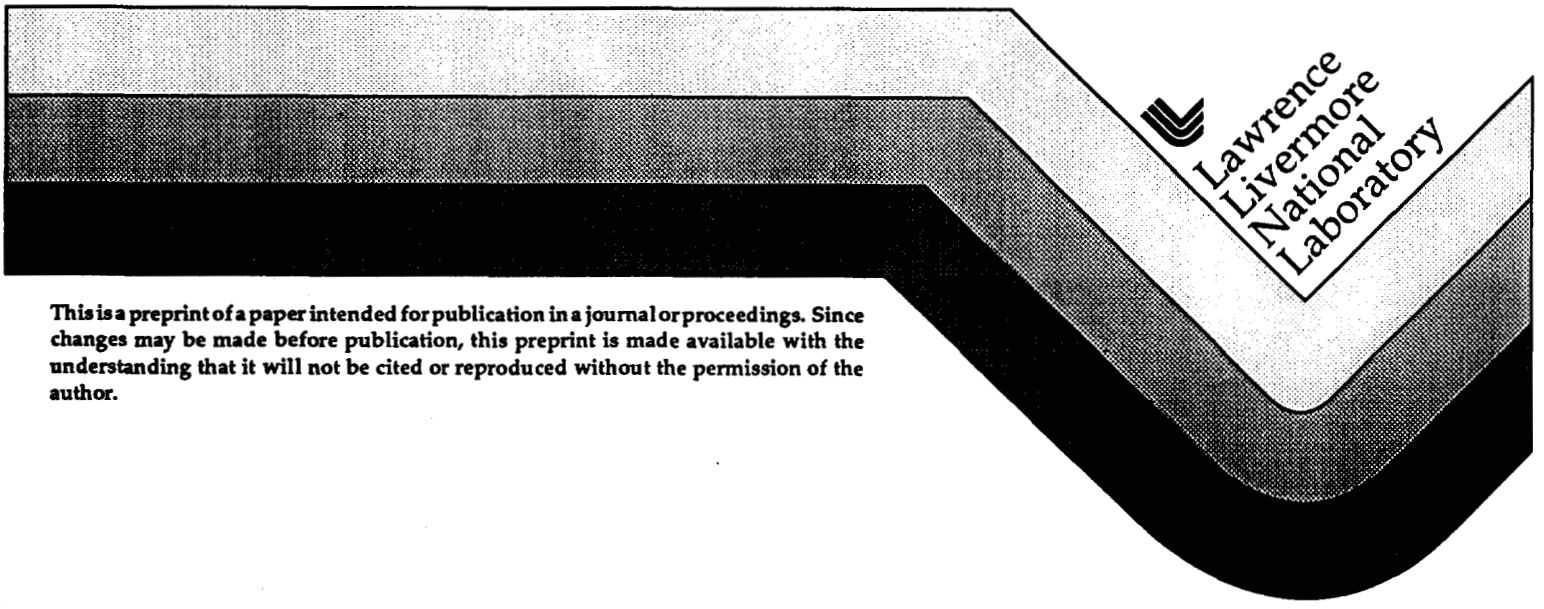

Numerical simulation of ultra-short laser pulse energy deposition and transport for material processing*

A.M.Rubenchik, M.D.Feit, M.D.Perry, J.T.Larsen†

Lawrence Livermore National Laboratory,

P.O.Box 808 MS L-449

Livermore, CA 94550

†Cascade Applied Sciences,Inc.

P.O.Box 4477

Boulder, CO 80306

Abstract

We have extended the physics of the one dimensional radiation hydrodynamics simulation code HYADES to include processes important for studying laser-matter interaction in the eV and sub-eV range with dielectrics and metals. Ultra-short laser pulses are advantageous in many materials processing situations where most of the absorbed laser energy appears in mass motion, and little appears as thermal energy. Major additions to the code include 1) the transport, reflection and absorption of laser light, 2) thermal energy transport and improved shockwave physics, and 3) improved models for the equation of state, strength of materials, and fracture. Examples from materials processing and plasma generation were chosen for simulation. Our

numerical simulations include the effects of radiation transport, hydrodynamic expansion and shockwave phenomena.

* Work at Lawrence Livermore National Laboratory performed under the auspices of the U.S. Department of Energy under contract No. W-7405-ENG-48.

I. Advantages of material processing with ultra-short laser pulses(USLP)

Recent ultra-short laser pulse (USLP) irradiation experiments on a variety of materials have demonstrated distinct advantages for material processing. These subpicosecond laser pulses cause the laser energy to be deposited in a very thin layer (of order a few skin depths) of material, thus creating an inertially confined high energy density plasma. This plasma is then ejected by the plasma pressure on a hydrodynamic timescale which is much shorter than the thermal conduction timescale which transports heat inward. As a result collateral damage is minimal.

A particular advantage is that USLPs can be used for processing transparent materials. At high intensity multiphoton ionization and subsequent electron avalanche produce a sufficient density of electrons for effective light absorption in any material. The nonlinear nature of the laser absorption process in dielectrics leads to a sharp ablation front; thus, one can use this process for very precise material processing. Because of the short pulse duration, plasma shielding is absent for USLP irradiation and the

ablation efficiency is high when compared to that of pulses of nanosecond duration.

The choice of optimal laser parameters involves balancing effects of pulse duration, intensity, repetition rate, beam structure, prepulse, etc. Since optimization of laser parameters by laboratory experiments is time consuming, it is important to develop models to aid this task. In addition, one gains valuable insight into the physical processes of laser-material interactions from the numerical simulations. However, because many physical processes are involved, sophisticated numerical tools must be developed. High intensity laser radiation causes strongly localized absorption, thus producing enormous pressure and concomitant temperatures. This high energy density plasma is subsequently relaxed by shock wave generation, radiative transport and plasma expansion (PdV cooling). Moreover, even during the time of the USLP irradiation, the absorption characteristics change with plasma density and temperature and must be described in self-consistently. To properly describe all of the above physics processes, which are governed by nonlinear, coupled differential equations, modeling must be done with a radiative hydrodynamic computer code properly adapted to the description of the USLP interaction with matter.

The short pulse duration greatly simplifies modeling. Even on the nanosecond time scale ejecta typically expand much less than the laser spot size so a one dimensional treatment is adequate .

We have used the HYADES [1] code, which fits the above requirements, for our simulations of laser material processing with USLP.

II. Features of the HYADES radiation hydrodynamics simulation code.

HYADES is a one-dimensional, three geometry (planar, cylindrical, or spherical), three fluid, radiation hydrodynamics simulation code. The conservation equations for mass, momentum and energy are solved in a Lagrangian coordinate system, which means that the computational mesh is "frozen" in the fluid and moves with it; this method is well suited for materials which may undergo density changes of several orders of magnitude during the course of a simulation; this happens in the vicinity of the material heated by the laser. The three fluids (electrons, ions, and radiation) are treated individually in a fluid approximation, each having its own temperature.

In addition, they are loosely coupled to each other and thus exchange energy. Each fluid is assumed to be in local thermodynamic equilibrium (LTE), which is to say that the electrons and the ions are described well in the classical limit by Maxwell-Boltzmann statistics, and the radiation field is approximately Planckian. Electron degeneracy effects are important in low temperature, high density plasmas, are taken into account.

The equation of state (EOS) quantities and related thermodynamic coefficients are obtained from external tables that have been formed using experimental data and/or theoretical models. The user has a choice of

ionization models including Saha, Thomas-Fermi, and an LTE average-atom model, or a time-dependent nonLTE model. Energy transport by free electrons and ions is modeled in the flux-limited diffusion approximation. Radiation is transported according to the photon energy; ultra-violet and soft xrays have very short mean free paths while the more energetic photons will penetrate deeply into the material; the absorption (and emission) coefficients are determined self- consistently from the atomic physics model of choice, or they may be supplied by the user in tabular form. Absorption of laser light by a hot plasma is often dominated by inverse bremsstrahlung, with parametric processes contributing to the absorption under certain plasma conditions and laser conditions.

III. Extensions to HYADES with models relevant to material processing.

The absorption of USLP light in solid materials takes place in a thin layer. Since there is essentially no change in the density of this layer during the course of the irradiation, the absorption fraction is given by the Fresnel equations. This is appropriate since the wavelength of the light is long compared to the electromagnetic skin depth. The absorbed fraction is given by

$$\alpha = 1 - \left| \frac{1-\sqrt{\varepsilon}}{1+\sqrt{\varepsilon}} \right|^2$$

$$\approx 4\,\mathrm{Re}(\sqrt{\varepsilon}\,)/|\varepsilon| \approx 2\frac{\nu}{\omega\sqrt{\frac{n}{n_c}}}; \qquad \nu << \omega$$

Plasma absorption in our simulations was described within the Drude model. The dielectric constant of material is given by the expression

$\varepsilon = 1 - \frac{\omega_p^2}{\omega(\omega + i\nu)}$ where $\omega_p = [ne^2/m_e e_0]^{1/2} = 5.6 \times 10^4 \sqrt{n}$ Here ω_p and ω are the plasma frequency and frequency of light, respectively, n (in cm^{-3}) is the electron density, n_c is the critical plasma density at frequency ω and ν is the electron-ion collisional frequency. One can see that for high collisional rates absorption is high even when the plasma density is much larger than critical.

This model is adequate for any material at high temperatures. For metals, it is reasonable at low temperatures with the ionization level described by the Thomas-Fermi model. For dielectrics, we can assume that at the pulse front multiphoton ionization instantly creates the plasma layer. A more self-consistent model [2], including multiphoton ionization as given by the Keldysh formula and impact ionization can be used.

The electron-ion collision frequency for a dense cold plasma was taken as a constant comparable to the light frequency because there are no more reliable estimates for cold, dense plasma. For a review of this subject along with some estimates see e.g.ref [3]. In our simulations, we have used the cold collision frequency as an adjustable parameter to match the absorbed laser energy to experimental data. Because there is no plasma motion during the laser pulse, the plasma temperature rises rapidly, and the collision frequency is well described by the Spitzer model for an ideal plasma. As a result, the

absorption efficiency decreases during the course of the irradiation. This effect is most important for laser pulses of high intensity.

Some industrial applications involve the processing of metal covered by a thin dielectric film, such as water. The transparent dielectric is used to confine ejected material, thus increasing the pressure and ablation rate at the material surface. As laser energy is absorbed, dielectric material adjacent to the interface is heated, and becomes ionized. Laser energy is then absorbed in this heated dielectric layer which in turn heats an adjacent layer. The result is a laser supported ionization wave propagating back toward the laser. This wave shields the material which was supposed to be irradiated. Such situations can be modeled by HYADES with user specified temperature dependent absorptive index and thermal diffusivity.

IV. Simulations of USLP interaction with dielectrics and metals

In Figs(1,2) the pressure and temperature resulting from interaction of a 0.5 ps Gaussian pulse with a fused silica surface are shown. The pulse intensity, 0.5 PW /cm^2 (1 PW=10^{15} W) is high enough to ionize atoms at the very front of the pulse. Absorbed energy produces high temperature and pressure in a very narrow layer of material. One can see that very little plasma expansion occurs during the pulse. This justifies the use of the Fresnel model for plasma absorption. One sees this is not true for pulses with duration of even a few picoseconds since the plasma corona formation takes place on this time scale. One sees also that the high temperature zone is convected out with ejecta explaining the small collateral damage for USLP

processing. The shock launched into the material can be seen in Fig.(1). The amplitude of the shock is initially very high but decays over a few microns. The high pressure zone is also convected away with the ejecta.

The decrease in collision frequency at high temperature sharply increase the reflectivity and a plasma mirror phenomena occurs[4]. In the example considered here, the total reflectivity was over 90% in good agreement with experiment[5].

As mentioned above there are no reliable estimates for the collision rate in a cold , dense plasma. Fortunately, at the high intensity considered above, the result is not sensitive to the initial absorption. For example, higher initial absorption results in faster plasma heating and absorption termination. For intensities an order of magnitude smaller, the reflectivity is sensitive to the cold plasma collisional rate and comparison with experiments can be used to study the physics of highly non-ideal plasma.

It is clear that the plasma mirror effect is general and occurs for any material. This explains the well known experimental fact that the USLP ablation efficiency decreases with increasing intensity.

We compared Al ablation by USLP and nanosecond pulses. Pulse energies were chosen to correspond to comparable amounts of ablation. Because the intensity of the USLP is much lower than in the previous example, the plasma mirror effect is unimportant. Absorbtion and ablation efficiency is high. The calculations clearly demonstrate the advantages of USLP material processing. For USLP processing the zone of high temperature

convects out with ejecta, a small amount of shock heating is observed. For the longer,, nanosecond pulse, the heated zone expands inward resulting in higher collateral damage.

Another confirmation of minimal collateral damage is shown in Fig.(3). Here we plot the fraction of absorbed energy carried out as kinetic energy of ejecta for the USLP and nanosecond pulses. The remainder of the energy is either deposited in the bulk as heat and material damage or radiated away (a few percent). One sees that for the USLP, where the total amount of absorbed energy is much smaller than for the longer pulse, only a small fraction remains in the material. For the longer pulse, most of the absorbed energy is transferred to the bulk producing collateral damage.

Figs.(4,5) show the density and pressure resulting from the interaction of a 10.7 J/cm^2 , 1.06 μm, 10 ps pulse with a 20 μm thick stainless steel film. More than 30% of the incident energy was absorbed. The results are plotted in Lagrangian coordinates. The first zone thickness was 8 nm with subsequent increase of zone thickness by 5% per zone. One sees in Fig.(4) the evolution of a sharp boundary between ablated and nonablated material. The ablated thickness is about 50 nanometers.

Material is compressed behind the inward propagating shockwave. The shock is reflected at the free boundary at about 5 ns. Fig.(5) shows the corresponding pressure evolution. The shock rapidly attenuates as it propagates inward. Tensile stresses (negative pressure in Fig.(5)) produced in the material can result in spallation. In the present example, the tensile

stress is a few tens of kbars which is sufficient for spallation. The spallation threshold and the size of the spalled zone can be rougly estimated from such calculations. For a more quantitative prediction of spallation , the description must include a model of material strength.

Conclusion

We demonstrated the ability to simulate the interaction of intense laser pulses of duration from hundreds fs up to a few ns with with dielectrics and metals. Comparison studies of USLP and ns pulse ablation reproduce the experimentally observed higher ablation efficiency and smaller collateral damage for the USLP. Directions for improved simulations were indicated.

References

1 J.T. Larson, "HYADES - A Radiation Hydrodynamics Code for Dense Plasma Studies," in *Radiative Properties of Hot Dense Matter*, edited by W.Goldstein, C. Hooper, J. Gauthier, J. Seely and R. Lee (World Scientific, Singapore, 1991)

2. B.C. Stuart, M.D. Feit, M.D. Perry, A.M. Rubenchik, and B.W. Shore, Phys. Rev.Lett., 74, 2248, (1995); ibid, Physical Review B, 53, 1749 (1996).

3. R.M.Moore, "Atomic physics of laser-produced plasmas". In *Physics of Laser Plasma.*, Edited by A.Rubenchik, S.Witkowski North-Holland 1991

4. L.Spitzer Jr., *Physics of fully ionized gases*, Wiley Interscience, New York 1967

5. "Plasma Mirrors", M.D. Perry, V. Yanovsky, M.D. Feit, A.M. Rubenchik, LLNL report UCRL-JC-125376, 1997 (sub. Phys. Plasma))

Figure captions

Figure 1: Evolution of pressure due to a 500 fs, 0.5 PW/cm^2 pulse incident on fused silica. Distance z measured into the substrate is positive.

Figure 2 Evolution of temperature due to a 500 fs, 0.5 PW/cm^2 pulse incident on fused silica. Peak intensity occurs at time t=1 ps.

Figure 3 Fraction of absorbed energy appearing as kinetic for USLP and ns pulse ablation of Aluminum

Figure 4 Density evolution for ablation of stainless steel film 10 ps pulse. Distance is plotted in Lagrangian coordinates.

Figure 5 Pressure evolution for ablation of stainless steel film. View from the rear side. Shock pressure rapidly decays from 1Mbar to few tens of kbar on the film boundary. Shock reflection from the free surface and consequent tensile stress (negative pressure) generation is visible.

Figures

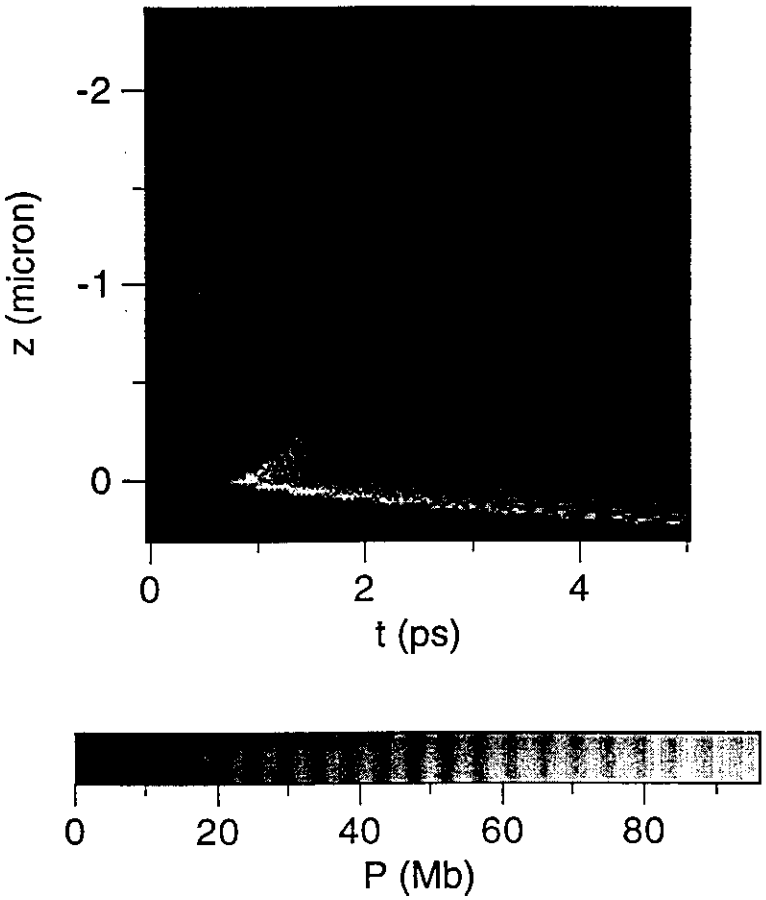

Fig. 1

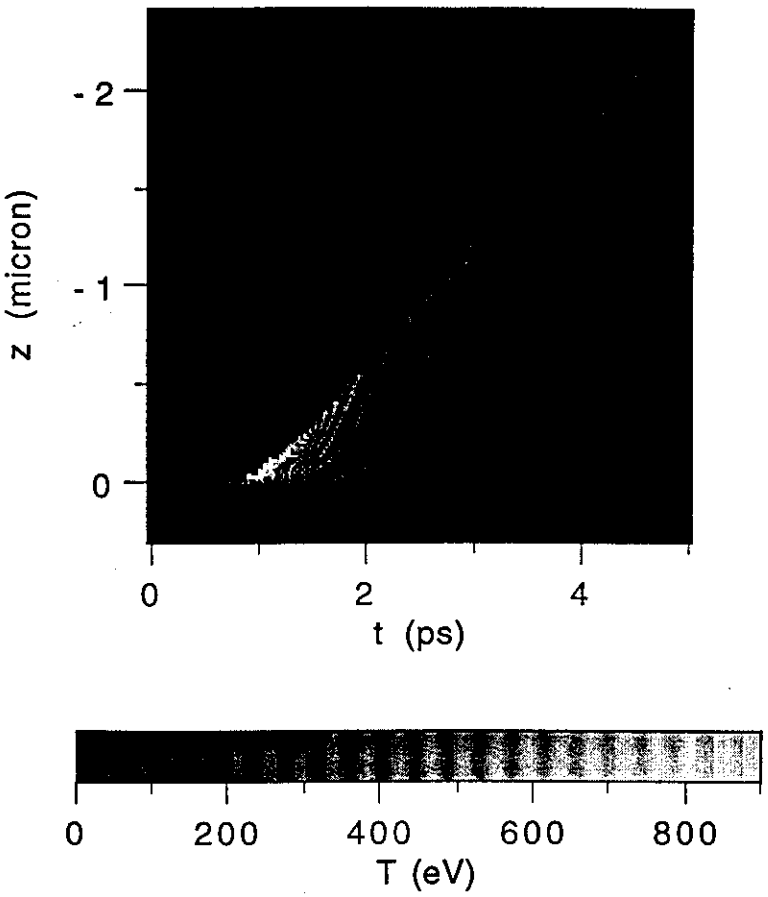

Fig. 2

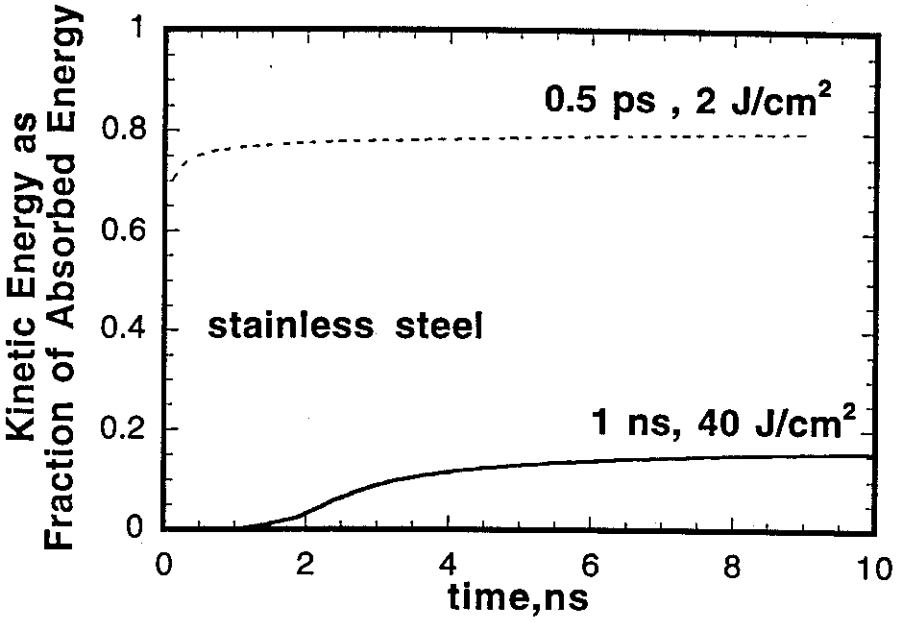
Kinetic Energy as
Fraction of Absorbed Energy
1
0.8
0.6
0.4
0.2
0
0.5 ps , 2 J/cm²
stainless steel
1 ns, 40 J/cm²
0
2
4
6
8
10
time,ns

Fig.3

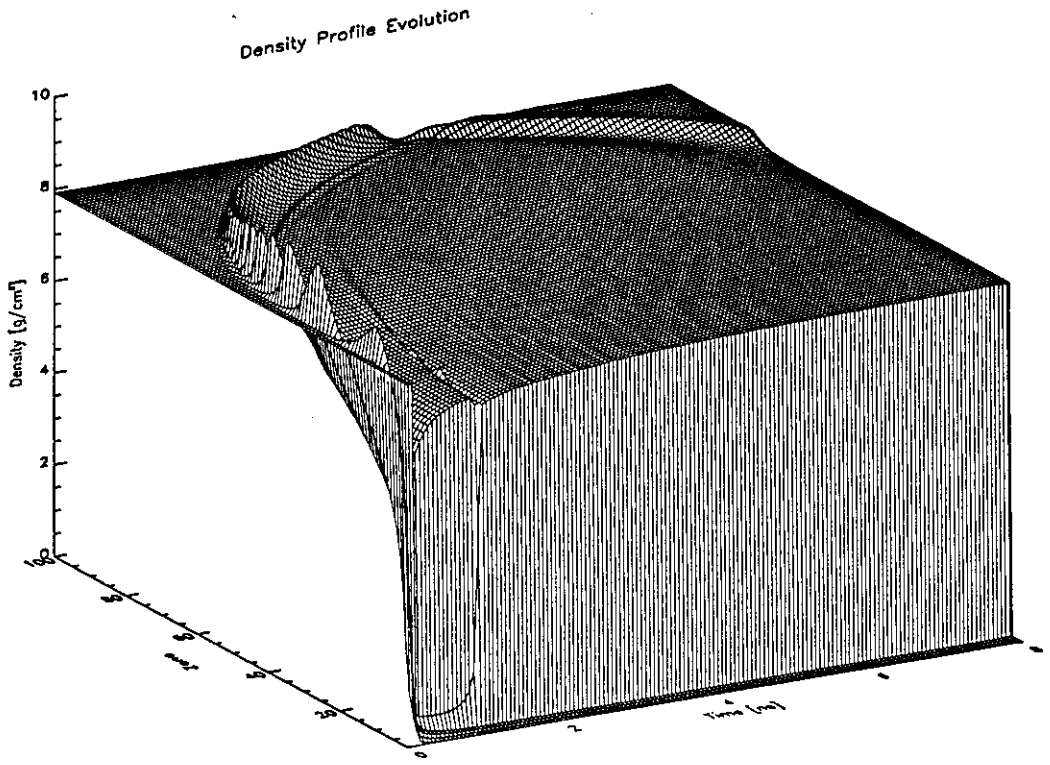
Density Profile Evolution
Density [g/cm³]
10
8
6
4
2
0
Time [ns]

Fig.4

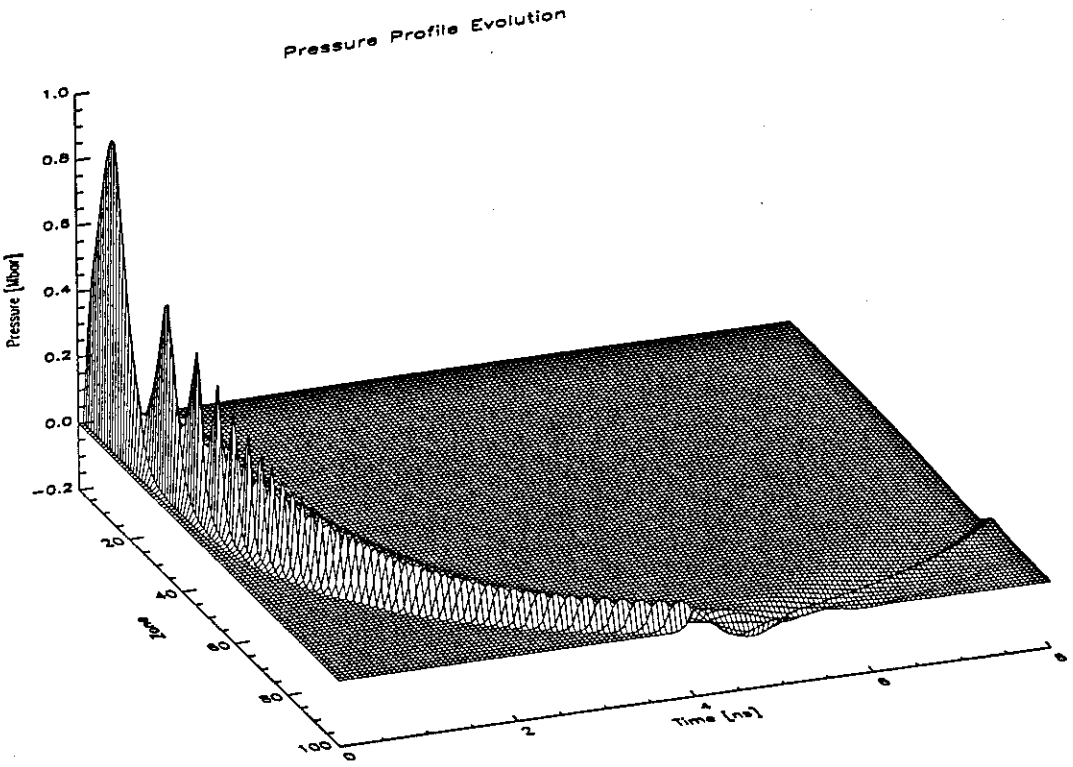
Pressure Profile Evolution
Pressure [Mbar]
1.0
0.8
0.6
0.4
0.2
0.0
-0.2
Time [ns]
0
2
4
6
8
Zone
20
40
60
80
100

Fig.5

Technical Information Department • **Lawrence Livermore National Laboratory**
University of California • Livermore, California 94551